viously discussed by F. Krmpotic and D. Tadic, Phys. Letters 21, 680 (1966). Their interpretation, however, is different from ours. See, also, the second paper in Ref. 5.

[9]M. J. Goldberger and S. B. Treiman, Phys. Rev. 110, 1178 (1958).

[10]S. Adler, Phys. Rev. 139, B1638 (1965). This approach was followed for the vector current in the second paper in Ref. 5.

[11]See the first paper in Ref. 5, and references therein. See, also, E. J. Konopinski, *The Theory of Beta Radioactivity* (Clarendon Press, Oxford, England, 1966).

[12]J. Sodermann and A. Winther, Nucl. Phys. 69, 369 (1965).

[13]We have assumed that $F_A(0) \neq 0$ and $f_{\pi if}(0) \neq 0$.

[14]Y. Nambu, Phys. Rev. Letters 4, 380 (1960).

[15]See the second paper in Ref. 1.

[16]For β^+ decay, C is negative so that a more careful analysis is necessary.

[17]We have assumed that $f_1(0) \neq 0$ and $f_{\pi if}(0) \neq 0$. It should be noted that if $f_1(0) = 0$, an entirely different result follows.

[18]Note that in Eq. (76) the contribution of the f_2 term appears to be $[W_0/(m_i + m_f)](f_2/f_1)$, but when combined with the lepton part, it is $[m_e/(m_i + m_f)](f_2/f_1)$.

[19]See T. Nagarajan, M. Ravindranath, and K. Venkata Reddy, Nuovo Cimento 3A, 699 (1971) for the latest list of references.

[20]A preliminary discussion of these results appears in Phys. Letters 41B, 39 (1972).

PHYSICAL REVIEW C VOLUME 6, NUMBER 6 DECEMBER 1972

Study of ^{15}N States by the ^{14}N(d, p) Reaction

A. Amokrane, M. Allab, H. Beaumevieille, and B. Faid
Institut d'Etudes Nucléaires d'Alger, Algérie

and

O. Bersillon, B. Chambon, D. Drain, and J. L. Vidal
Institut de Physique Nucléaire, 69-Villeurbanne, France

(Received 1 August 1972)

The bound states of ^{15}N have been studied by the ^{14}N(d, p) reaction. Absolute differential cross sections were measured at $E_d = 3$ MeV for the 9.05-, 9.152 + 9.155-, 9.22-, 9.76-, and 10.07-MeV states and at $E_d = 3.6$ MeV for the 9.76-, 9.83-, 9.93-, 10.07-, and 10.45-MeV states in ^{15}N. The target was natural nitrogen confined in a differentially pumped gas target. Distorted-wave Born-approximation analysis and Hauser-Feshbach calculations indicate that $l_n = 1$ is involved in the formation of the 9.22-, 9.76-, and probably 10.45-MeV states, whereas $l_n = 2$ transfer is associated with the 9.155-MeV level. An $l_n = 0$ transfer was discerned for the angular distribution associated with the 9.05-MeV state and $l_n = 0 + 2$ for the angular distribution associated with the 10.07-MeV and probably the 9.93-MeV ^{15}N state. Spectroscopic factors have been obtained. The correspondence between mirror levels in ^{15}N and ^{15}O and those predicted within the framework of the weak-coupling model is discussed.

I. INTRODUCTION

In recent papers,[1,2] the negative- and positive-parity states for $A = 15$ have been investigated in a weak-coupling model. The over-all agreement with experimental energies, structure information from direct reactions, and electromagnetic transitions is good for all the known levels below 10 MeV. In addition, several predictions have been made and a one-to-one correspondence between all levels of the $A = 15$ nuclei below 10-MeV excitation energy is suggested. This implies spin and parity assignments of $\frac{5}{2}^+$ for the $J = \frac{5}{2}$ member of the 9.16-MeV doublet, $\frac{1}{2}^-$ for the 9.22-MeV level, and $\frac{3}{2}^-$ for the other member of the 9.16-MeV doublet.

The experimental spectra[3] for ^{15}N and ^{15}O and the positive- and negative-parity states below 10.5 MeV predicted by Lie *et al.*[1,2] are shown in Fig. 1.

The present work was undertaken to complement experimental information on neutron transfer to ^{15}N states between 9.05 and 10.45 MeV and to clarify the spin-parity assignment of these states. Many experimental studies have previously been reported on the ^{14}N(d, p) reactions and corresponding information is compiled in Ref. 3. In particular, a recent investigation[4] of the ^{14}N(d, p) reaction was devoted to levels up to 10.80 MeV excitation in ^{15}N. However, very few experimental data have been reported on the levels in ^{15}N near 9 MeV excitation, probably owing to experimental difficulties associated with the contaminants present in solid targets which obscured these levels. In the

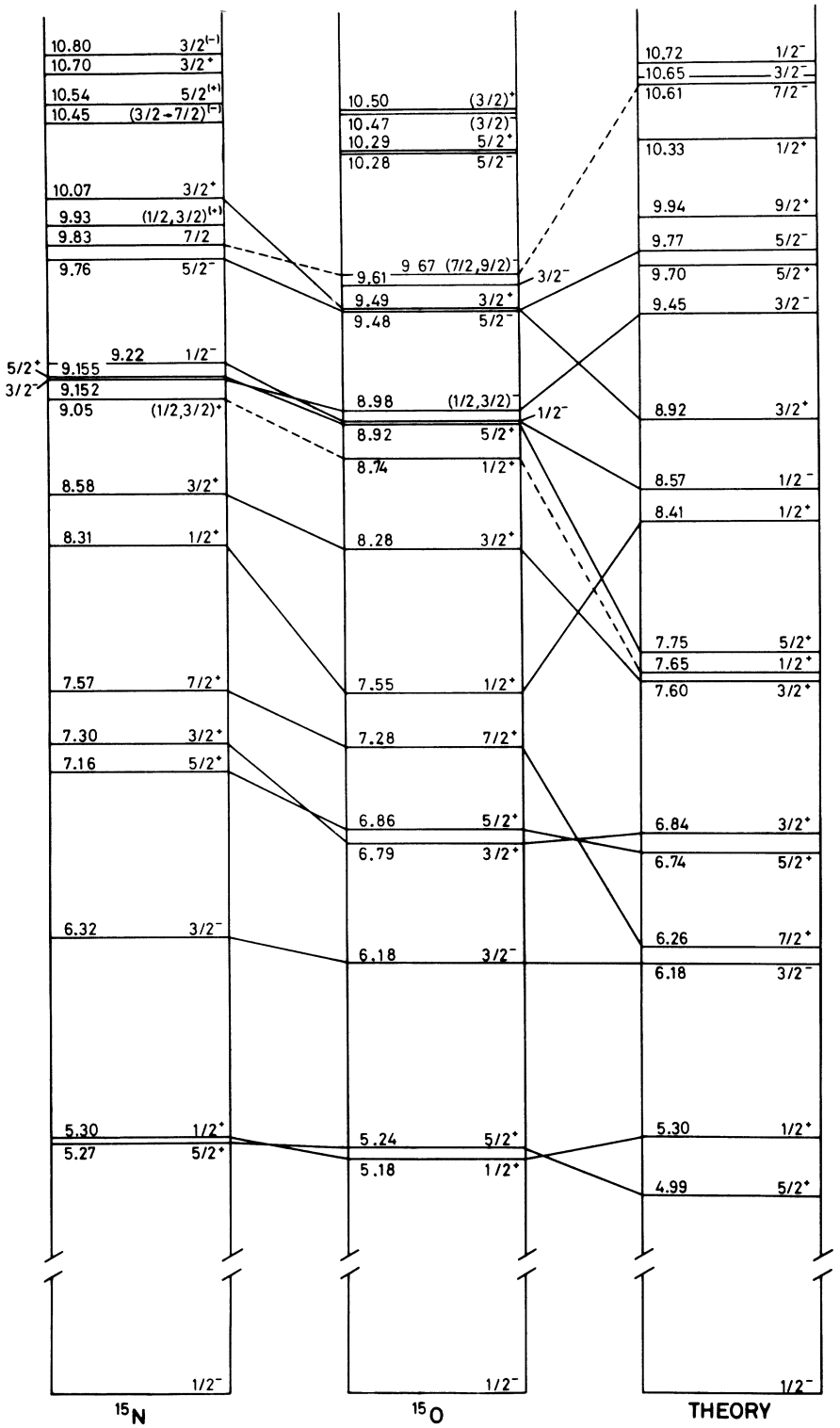

FIG. 1. Energy-level diagrams for ^{15}N and ^{15}O, showing the excitation energies and spin-parity assignments as reported from previous measurements and from the present work. The data are taken from the compilation of Ajzenberg-Selove (Ref. 3) and incorporate the results of later measurements as explained in the text. The theoretical spectra are those calculated by Lie *et al.* (Refs. 1 and 2).

present work, l_n values and spectroscopic factors for ^{15}N states have been extracted from distorted-wave Born-approximation (DWBA) fits to the measured ^{14}N$(d,p)^{15}$N stripping cross sections.

The experimental procedure used in this experiment is described in Sec. II. Experimental results are reported in Sec. III, while the DWBA analysis is discussed in Sec. IV. Section V shows the DWBA fits to the experimental angular distributions while the results for each final state of ^{15}N are presented. The extracted (d,p) spectroscopic factors are reported in Sec. VI. A comparison of experimental findings concerning the properties of the ^{15}N nuclear structure with the predictions of weak-coupling model and with the corresponding quantities for the isobaric analog states of ^{15}O is presented in Sec. VII.

II. EXPERIMENTAL PROCEDURE

The experimental data reported here were performed at incident deuteron energies of 3 MeV with the Alger 3-MeV Van de Graaff accelerator, and at 3.6 MeV with the Lyon Haefely accelerator. The details of the experimental setup have been described previously.[5] A gaseous target of natural nitrogen (99% ^{14}N) has been used in a differentially pumped gas scattering chamber. The gas pressure used in the experiments was approximately 5 Torr. The beam current was measured in a collector under a molecular vacuum, separated from the scattering chamber by a 1-μm-thick nickel foil. The reaction particles were detected with a 8-μm-ΔE-1000-μm-E solid-state detector telescope employed in conjunction with a digital identifier system.[6] The system used allowed the detection and the identification of protons between 1.5 and 3 MeV. The total energy resolution was about 35 keV, allowing the separation of all the proton groups. A single monitor detector was fixed at a lab angle of 165°. The proton spectra observed with this detector were recorded simultaneously with the angular-distribution spectra.

The absolute differential cross sections of the ^{14}N(d,p) reaction were determined by normalizing the ^{14}N(d,p) yields to the yields for the elastic scattering of 1.00-MeV protons from argon which obeys the Rutherford-scattering law. The 1.00-MeV p-scattering experiment was carried out under the same conditions of pressure and beam integration current. Thus we were able to obtain absolute ^{14}N(d,p) cross sections directly from the known Rutherford-scattering cross sections.

III. RESULTS

A proton spectrum for $E_d = 3$ MeV recorded at an angle to the beam of 28° by using the digital identifier system is shown in Fig. 2, with the peaks labeled according to the final-state excitation energies in ^{15}N. The proton angular distributions were measured over the angular range $\theta = 15$ to 165° in the lab frame and are displayed in Figs. 3 to 10. The experimental errors are due to uncertainties in gas pressure, beam integrator current, and the normalization to the ^{40}A(p,p) results; these include statistical and estimated errors due to background subtraction and overlapping peaks. Thus, the over-all precision is about 10% except for forward-angle measurements where the uncertainties have to be increased. The calculated experimental uncertainties are shown in the figures.

IV. ANALYSIS

The theoretical curves are composed of an incoherent superposition of direct-reaction (DR) and compound-nucleus (CN) cross sections:

$$\frac{d\sigma}{d\Omega} = \left(\frac{d\sigma}{d\Omega}\right)_{\mathrm{DR}} + R\left(\frac{d\sigma}{d\Omega}\right)_{\mathrm{CN}}. \tag{1}$$

The compound-nucleus contribution is obtained from a Hauser-Feshbach calculation. However, a complication arises in the calculation of the compound-nucleus cross sections due to the presence of the direct-interaction contributions of the reaction channels that remove flux from the elastic channel before it can enter the compound nucleus.[7] The Hauser-Feshbach calculation overestimates, therefore, the compound-nucleus cross sections since it depends also on an accurate accounting of all the allowed exit channels from the compound nucleus. The reduction factor R was treated as an empirical normalization factor for the compound-nucleus contributions; it was de-

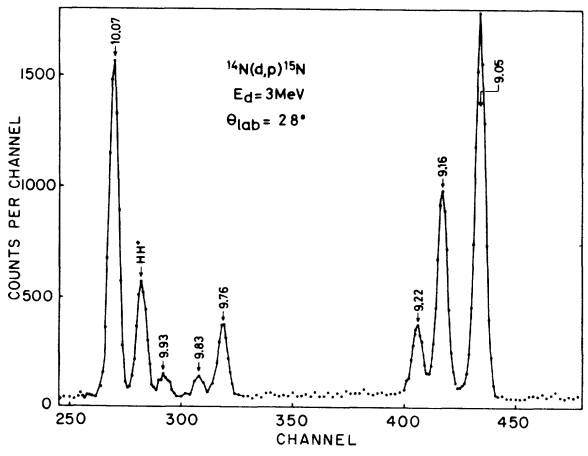

FIG. 2. Proton spectrum of the ^{14}N$(d,p)^{15}$N reaction at $\theta = 28°$ and $E_d = 3$ MeV, using the digital identifier system. The arrows indicate the positions of known levels in ^{15}N.

termined by matching the calculated Hauser-Feshbach cross section to the experimental cross section for the 6.32-MeV state, which does not contain any discernible direct component. The value of R thus obtained ($R=0.40$) was then used for all other transitions; the same value was also deduced from the Hauser-Feshbach calculation of total cross sections for the ^{14}N(d,α_{0-3}) reactions.[8,9]

A. Optical Potentials

The optical potentials used to calculate the distorted waves and the transmission coefficients have the form

$$U(r) = -Vf(r) - iWg(r) + V_C(r),$$

where $V_C(r)$ is the Coulomb potential with the nuclear radius fixed at $1.4A^{1/3}$ fm, and V and W the real and imaginary potential depths. The form factor $f(r)$ has the Woods-Saxon form; $g(r)$ has also the Woods-Saxon form. The parameters of the potentials used are given in Table I; no spin-orbit terms were included in these potentials. The potentials called D_1 and D_3 were those obtained by fitting the data[10] of elastic scattering of deuterons by ^{14}N; the potential D_1 is very similar to the potential found by Dietzch *et al.*[11] and by Gomes Porto *et al.*[8] to fit the elastic scattering of deuterons by ^{16}O and ^{14}N, respectively. The potential D_2 has been used in the ^{14}N(d,p) experiment by Phillips and Jacobs.[4]

The proton optical-model parameter P_1 was used by Gallmann, Fintz, and Hodgson[12] and Smith and Ivash[13] and provides a good fit for the ^{16}O(d,p) reaction analysis. The parameter set P_2 was used by Phillips and Jacobs[4] for the ^{14}N(d,p) reaction analysis. The parameter set N was deduced by Wilmore and Hodgson[14] from the analysis of neutron elastic scattering cross sections for medium nuclei. The α optical-model parameter A was determined by Morand[9] from the analysis of α elastic scattering on ^{12}C.

B. DWBA Analysis

For the direct-reaction calculation, the distorted-wave program written by Nguyen Van Sen[15] was used. The wave function of the neutron stripped in the (d,p) reaction was calculated from a potential well of the Woods-Saxon shape. The radius parameter of the well was 1.25 fm; the diffuseness parameter was 0.65 fm and no spin-orbit term was considered. The magnitude of the bound-neutron potential was varied to reproduce the binding energy of the stripped neutron [$B(n)=Q(d,p)+2.225$ MeV]. Since a spin-1 target was used, the l_n value is not always unique, and terms with $l_n=0$ and 2 both contribute for positive-parity levels of spin $\frac{1}{2}^+$ or $\frac{3}{2}^+$. However, for relatively low values of deuteron bombarding energy ($E_d \leq 3.6$ MeV), the compound-nuclear effects are anticipated to be important beyond about 80°; thus the $l_n=3$ strength was neglected in $\frac{3}{2}^-$ or $\frac{5}{2}^-$ states which were assumed consistent with a pure $l_n=1$ assignment.

The DWBA calculations for each transition considered were carried out with no radial cutoff. The combinations of potentials (D_1,P_1), (D_2,P_2), (D_3,P_1) yield reasonable fits for all the proton groups. The results of DWBA calculations with the different potentials are shown in Figs. 3 to 6 for the levels between 9.05 and 9.76 MeV. It is found that though there are appreciable differences between the calculated differential cross sections, the angular-momentum transfer is clearly well defined. In particular, the different potential sets give practically identical fits for the $l_n=1$ levels (see Figs. 5 and 6). The results of DWBA analysis on angular momentum transfer and spectroscopic factors are discussed in the following sections.

TABLE I. Optical-model parameters used in the DWBA and Hauser-Feshbach calculations. The real part V and imaginary part W of the potentials have a Woods-Saxon form:

$$f(r)=[1+\exp(r-r_vA^{1/3})/a]^{-1}, \quad g(r)=[1+\exp(r-r_wA^{1/3})/b]^{-1}.$$

Channel	Potential	V (MeV)	W (MeV)	r_v (fm)	a (fm)	r_w (fm)	b (fm)	Reference
$d+^{14}$N	D_1	76	10	1.4	0.7	1.4	0.7	10
	D_2	91.2	20	1.4	0.7	1.4	0.7	4
	D_3	123	15.23	1.762	0.7	1.736	0.57	10
$p+^{15}$N	P_1	64	5	1.25	0.5	1.25	0.5	10
	P_2	48.3	7	1.25	0.65	1.25	0.47	4
$n+^{15}$O	N	47	9.52	1.32	0.66	1.27	0.48	14
$\alpha+^{12}$C	A	160	30	1.22	0.66	1.22	0.66	9

V. RESULTS AND DISCUSSION

A. 9.05-MeV Level

The ^{15}N 9.05 → 0 transition was found to be $E1$,[16] requiring even parity. Proton-γ angular correlations from the ^{13}C(^{3}He, $p\gamma$)^{15}N reaction[17,18] give an isotropic distribution, in agreement with $J=\frac{1}{2}$ or $\frac{3}{2}$. No clear experimental data for the ^{14}N(d,p)^{15}N reaction have been reported for the 9.05-MeV state; the angular distribution measured by Green and Middleton[19] for the unresolved triplet of levels at 9.05, 9.152, and 9.155 MeV indicates $l_n=1$. The angular distribution displayed in Fig. 3 for the 9.05-MeV state at $E_d=3$ MeV indicates peaking at 0° and is well fitted by the $l_n=0$ DWBA curve implying positive parity. The present findings are in agreement with the recently reported results[20] of a ^{13}C(^{3}He, p)^{15}N study: The characteristic $L=1$ angular distribution in the ^{13}C(^{3}He, p) reaction implies positive parity for the 9.05-MeV state.

B. 9.152-9.155-MeV Levels

The 9.16-MeV doublet was not resolved in this experiment. The predominantly ground-state decaying member of this doublet ($E_x=9.152$ MeV) has been assigned[16] $J^\pi=\frac{3}{2}^-$. The spins of the two levels were established from triple angular-correlation measurements in the ^{14}C(p,γ) reaction.[21] These measurements indicate that the $\frac{3}{2}^-$ 9.152-MeV level is the second excited negative-parity state in ^{15}N. The other member of the 9.16-MeV doublet ($E_x=9.155$ MeV) is assigned $J=\frac{5}{2}$. The angular distribution for the ^{14}N(d,p) reaction, measured by Phillips,[4] can be fitted by either a combination of $l_n=1$ and 2, implying $\frac{3}{2}^+$ or $\frac{5}{2}^+$ for the 9.155-MeV state or a combination of $l_n=1$ and 3 implying $\frac{5}{2}^-$ or $\frac{7}{2}^-$. The angular distribution displayed in Fig. 4(a) for the 9.16-MeV doublet at $E_d=3$ MeV is fitted by the $l_n=2$ DWBA curve. The addition of a weak $l_n=1$ component gives a better fit [Fig. 4(b)], but the contributions from both $l_n=2$ and $l_n=1$ depend on the optical-model parameters used. However, the $l_n=2$ transition is predominant, implying positive parity for the 9.155-MeV state and thus $J^\pi=\frac{5}{2}^+$.

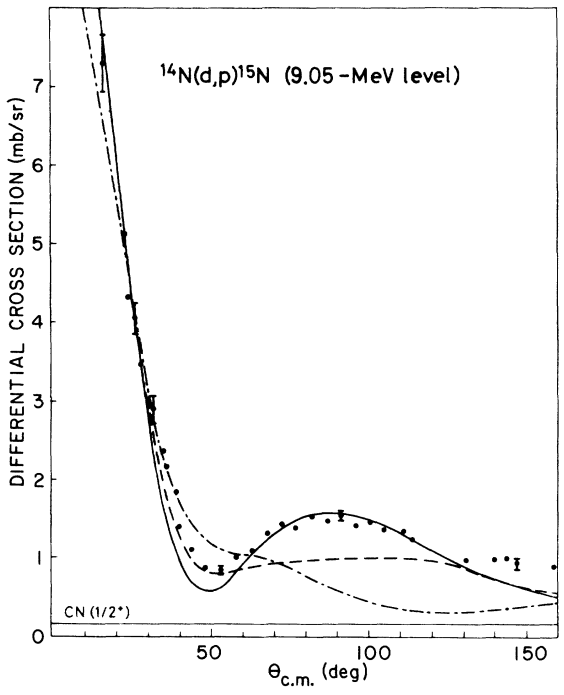

FIG. 3. ^{14}N(d,p)^{15}N angular distribution for the $(\frac{1}{2},\frac{3}{2})^+$ 9.05-MeV level at $E_d=3$ MeV. The solid, dashed, and dot-dashed curves represent $l_n=0$ DWBA fits (including the Hauser-Feshbach contribution) for (D_1,P_1), (D_3,P_1), and (D_2,P_2) potential parameters sets, respectively.

C. 9.22-MeV Level

Very little information is available for this level. Substantial discrepancies exist in the branching ratios for this state.[16,18] The lifetime limit $\tau<5\times10^{-3}$ sec[17] restricts the spin of the 9.22 MeV to $J\leq\frac{5}{2}$. This level is excited weakly by the ^{14}N(d,p) reaction. The angular distribution measured by Phillips and Jacobs[4] can be fitted about equally well by $l_n=1$ or $l_n=2$ so that the parity of this state is not determined. The angular distribution for the 9.22-MeV state displayed in Fig. 5 is well fitted at the forward angles by a DWBA curve which assumes $l_n=1$ transfer. An attempt was made to fit the experimental data under the assumption of $l_n=0$ or $l_n=2$ transfer. As is shown in Fig. 5, these assumptions lead to a very poor fit to the experimental data. It is thus concluded that the present findings completely remove the ambiguity as regards the orbital angular momentum transfer associated with the 9.22-MeV state. Consistent with this result, the 9.22-MeV state was discerned in the ^{13}C(^{3}He, p)^{15}N reaction to be formed via $L=1$ transfer[20]; from γ-γ angular correlation measurements of the 9.22-6.32-0 cascade decay, a preferred spin value of $\frac{1}{2}$ was found for this state.[20] In conjunction with these results, a $J^\pi=\frac{1}{2}^-$ assignment for this state appears confirmed.

D. 9.76-MeV Level

The limitation of $\frac{1}{2}^+$, $\frac{3}{2}^-$, or $\frac{5}{2}^-$ for the spin-parity of the 9.76-MeV level was derived from studies of the angular correlation of internal pairs in the 9.76 → 0 transition.[16] Proton-γ angular correlation measurements from the ^{13}C(^{3}He, $p\gamma$)^{15}N reaction imply $J=\frac{5}{2}$.[17,18] Only $J^\pi=\frac{5}{2}^-$ is consistent with these two measurements.

No experimental data for the ^{14}N(d,p) reaction have been reported previously for the 9.76-MeV level. Figure 6 presents the (d,p) angular distributions associated with this level at $E_d = 3$ and 3.6 MeV. The transition to the 9.76-MeV level shows a definite $l_n = 1$ stripping pattern well fitted by DWBA curves, implying negative parity in agreement with previous results.

E. 9.83-MeV Level

Proton-γ angular correlation measurements from the ^{13}C(^{3}He, $p\gamma$)^{15}N reaction require $J = \frac{7}{2}$.[17,18] There is no reported evidence concerning the parity assignment from the ^{14}N(d,p) reaction. The transition going to the 9.83-MeV level exhibits no stripping pattern (see Fig. 7). The very weak cross section can be accounted for by the compound-nucleus reaction mechanism.

F. 9.93-MeV Level

Internal-pair correlation measurements indicate $E1$ character for the ground-state transition[16] and thus $J^\pi = \frac{1}{2}^+$ or $\frac{3}{2}^+$. The angular correlation for the ground-state transition for the 9.93-MeV state is isotropic implying $J = \frac{1}{2}$ or $\frac{3}{2}$. The angular distribution for the ^{14}N(d,p) reaction measured by Phillips and Jacobs[4] can be accounted for predominantly by the compound-nucleus process with a combination of small $l_n = 0$ and 2 terms. The differential cross sections measured at $E_d = 3.6$ MeV were relatively weak (see Fig. 8) and the contribution of compound-nucleus processes is important. At forward angles $\theta \lesssim 70°$, this angular distribution can be fitted by the sum of $l_n = 0$ and $l_n = 2$ DWBA curves (see Fig. 8). However, within the large uncertainties in the data, a $l_n = 1$ assignment cannot be completely ruled out.

G. 10.07-MeV Level

Analysis of the angular correlation for the 10.07 $\rightarrow$ 0 transition from the ^{13}C(^{3}He, $p\gamma$) reaction[17,18] and internal-pair correlation measurements[16] give a definite $J = \frac{3}{2}^+$ assignment for this level. Figure 9 presents the (d,p) angular distributions to the 10.07-MeV level at $E_d = 3$ and 3.6 MeV. These angular distributions are well fitted by a combination of $l_n = 0$ and $l_n = 2$ transfers. The present findings are in agreement with the results obtained in the same reaction by Phillips and Jacobs.[4]

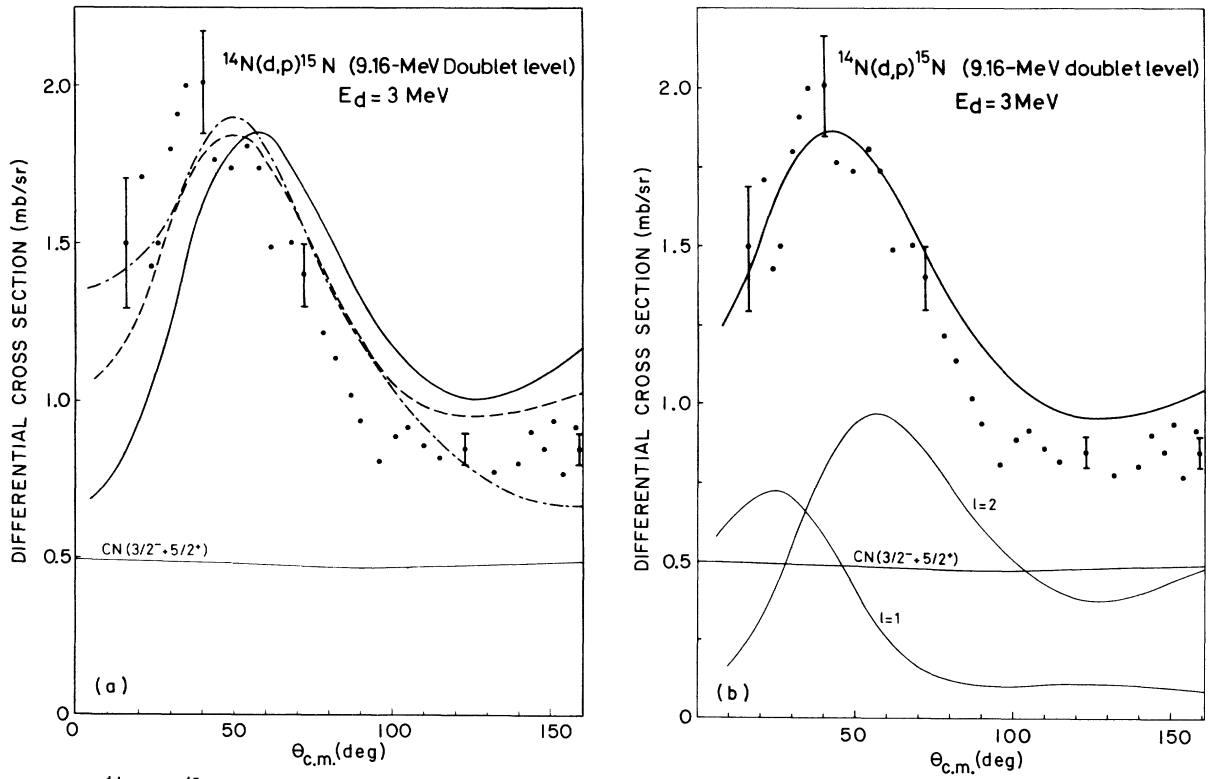

FIG. 4. ^{14}N(d,p)^{15}N angular distribution for the 9.16-MeV doublet level at $E_d = 3$ MeV. The solid, dashed, and dot-dashed curves of Fig. 4(a) represent $l_n = 2$ DWBA fits (including the Hauser-Feshbach contribution) for (D_1, P_1), (D_3, P_1), and (D_2, P_2) potential parameters sets, respectively. Figure 4(b) shows the sum of $l_n = 1$ and $l_n = 2$ DWBA fits (including the Hauser-Feshbach contribution) calculated with (D_1, P_1) combination.

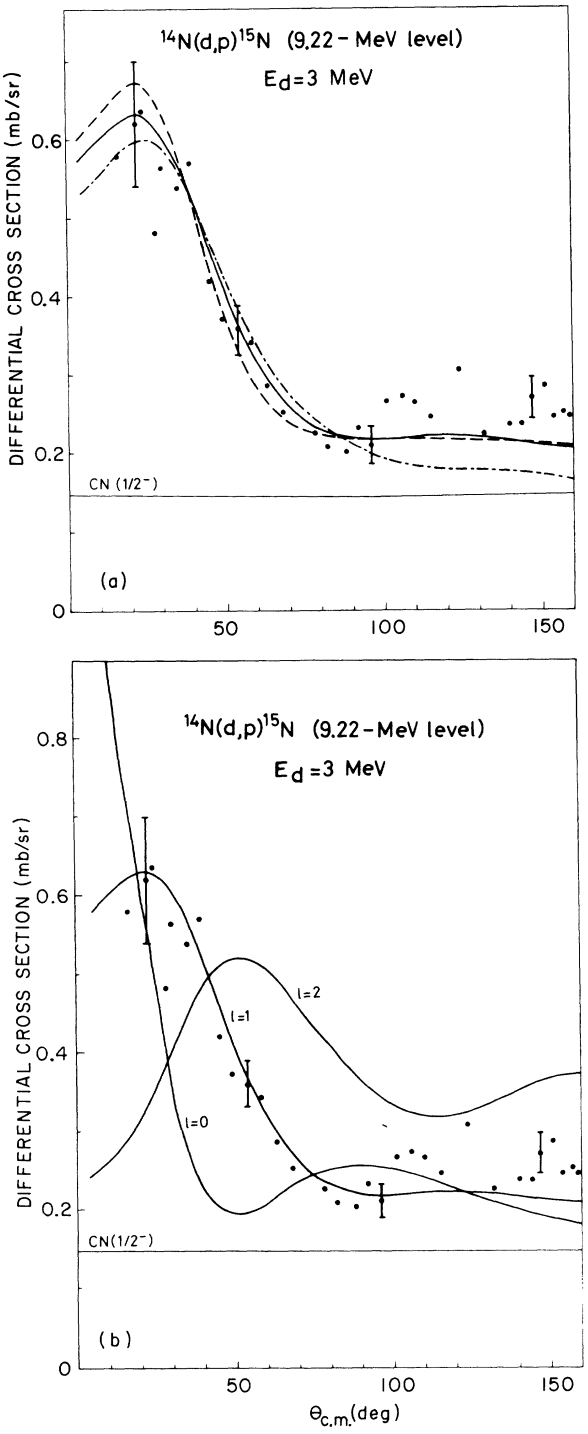

FIG. 5. ^{14}N(d, p)^{15}N angular distribution for the $\frac{1}{2}^-$ 9.22-MeV level at E_d =3 MeV. The solid, dashed, and dot-dashed curves of Fig. 5(a) represent l_n=1 DWBA fits (including the Hauser-Feshbach contribution) for (D_1,P_1), (D_3,P_1), and (D_2,P_2) potential parameters sets, respectively; Fig. 5(b) shows DWBA fits (including the Hauser-Feshbach contribution) for (D_1,P_1) combination and l_n =0, 1, and 2.

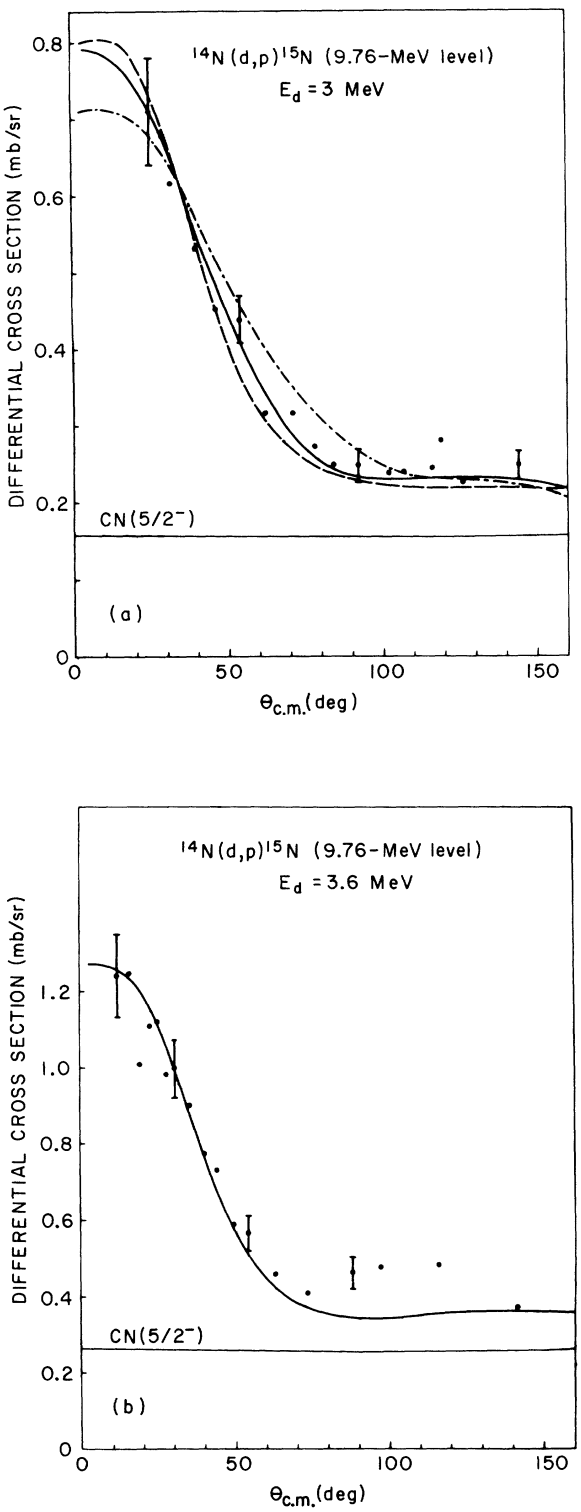

FIG. 6. ^{14}N(d, p)^{15}N angular distributions for the $\frac{5}{2}^-$ 9.76-MeV level at E_d =3 and 3.6 MeV. The solid, dashed, and dot-dashed curves represent l_n=1 DWBA fits (including the Hauser-Feshbach contribution) for (D_1, P_1), (D_3,P_1), and (D_2,P_2) potential parameter sets, respectively.

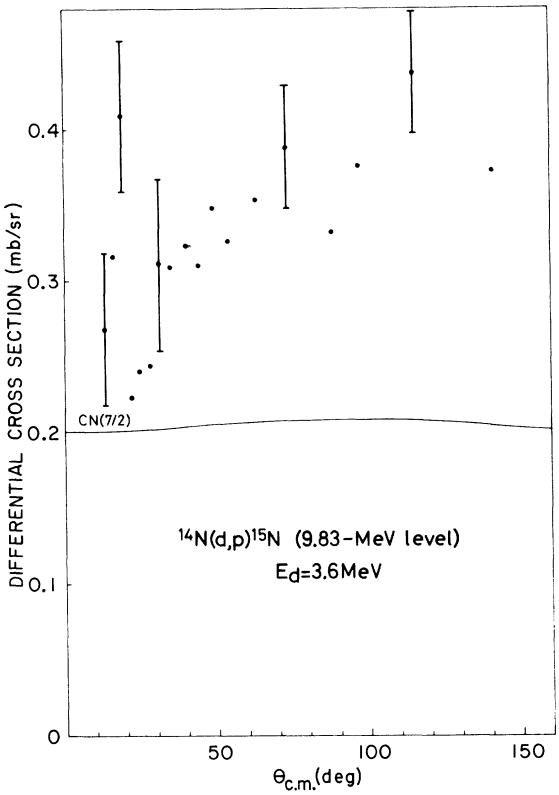

FIG. 7. ^{14}N(d,p)^{15}N angular distribution for the $\frac{7}{2}$ 9.83-MeV level at E_d = 3.6 MeV. The solid curve represents the Hauser-Feshbach contribution.

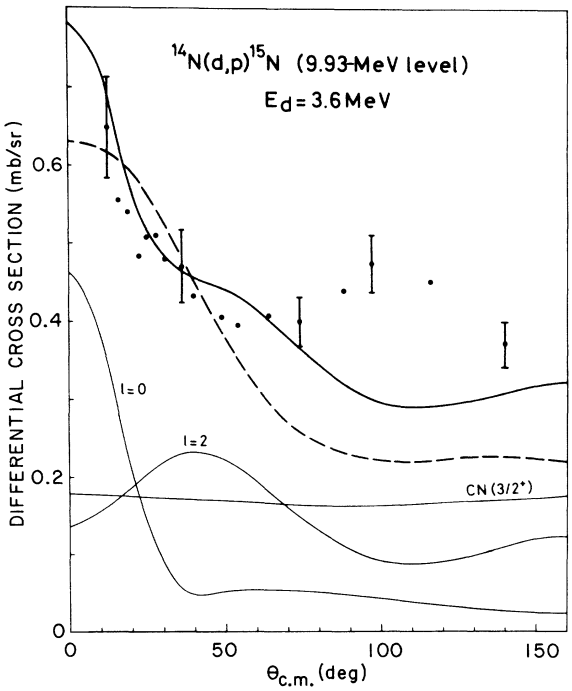

FIG. 8. ^{14}N(d,p)^{15}N angular distribution for the $(\frac{1}{2},\frac{3}{2})^+$ 9.93-MeV level. The solid curve represents the sum of l_n=0 and l_n=2 DWBA fits (including the Hauser-Feshbach contribution) calculated for (D_1,P_1) combination. The dashed curve represents l_n=1 DWBA fit (including the Hauser-Feshbach contribution) calculated for (D_1,P_1) combination.

H. 10.45-MeV Level

From angular-correlation measurements,[17] the possibilities $J=\frac{3}{2},\frac{5}{2},\frac{7}{2}$ remain as an assignment for the 10.45-MeV level. Phillips and Jacobs[4] report a very weak cross section for the ^{14}N(d,p) reaction. The angular distribution displayed in Fig. 10 is fitted by the l_n=1 DWBA curve. Because of the fact that compound-nucleus mechanisms contribute significantly in such a weak transition the assignment of the l_n value here must be regarded as tentative.

VI. SPECTROSCOPIC FACTORS

The spectroscopic factors were obtained from a comparison of the DWBA cross sections with the experimental data, after the compound-nucleus cross sections had been subtracted from the latter. The spectroscopic factors S for each state were obtained from the relation

$$\left(\frac{d\sigma}{d\Omega}\right)_{\text{exp}} = 1.65S\frac{2J_B+1}{2J_A+1}\left(\frac{d\sigma}{d\Omega}\right)_{\text{DWBA}}, \qquad (2)$$

where J_A and J_B are the spins of the initial and final states, respectively. The factor 1.65 has been suggested by Austern[22] to correct for Hulthen wave functions for the deuteron. The errors in the spectroscopic factors arise from the experimental uncertainties as shown by the error bars in figures and uncertainties in the DWBA and Hauser-Feshbach cross sections which depend on the optical-model parameters used. For the strongest transitions, the over-all uncertainty in the spectroscopic factors is ~20%. The estimated errors in some spectroscopic factors for weak transitions or those excited with two different values of angular momentum transfer may be up to 50%.

The spectroscopic factors were found to be rather insensitive to the choice of deuteron potentials: The use of potentials D_1-D_2 led to results that varied by less than 10%. The reliability of the results of the DWBA analysis is supported by the observation that the potential sets (D_1,P_1), (D_2,P_2) give spectroscopic factors close to unity,[4,10] for the 7.16-, 7.30-, 7.57-, and 8.31-MeV states in ^{15}N in agreement with the extreme single-particle shell model. The potential set (D_3,P_1) gives spectroscopic factors that are about 50% too high and was not used to extract spectroscopic factors. The

TABLE II. Spectroscopic factors for the reaction $^{14}N(d,p)^{15}N$.

E_x [a] (MeV)	J^π [c]	l_n		$(2J_f+1)S$		S	
		Reference d	Reference e	Reference d	Reference e	Reference d	Reference e
9.05	$(\frac{1}{2}, \frac{3}{2})^+$		0		0.30		0.15 [f]
9.152 [b]	$\frac{3}{2}^-$		1		0.128		0.032
9.155 [b]	$\frac{5}{2}^+$		2		0.78		0.13
9.22	$\frac{1}{2}^-$		1		0.090		0.045
9.76	$\frac{5}{2}^-$		1		0.126		0.021
9.83	$\frac{7}{2}$		No stripping				
9.93	$(\frac{1}{2}, \frac{3}{2})^{(+)}$	0	(0)		0.022		0.0054 [g]
		2	(2)		0.17		0.043 [g]
10.07	$\frac{3}{2}^+$	0	0	1.28	0.60	0.32	0.15
		2	2	1.92	2.56	0.48	0.64
10.45	$(\frac{3}{2}, \frac{5}{2})^{(-)}$		(1)		0.049		0.0082 [h]

[a] Reference 3.
[b] These two levels are not resolved and spectroscopic factors are extracted from the angular distributions fitted with the sum of $l_n=1$ and $l_n=2$ curves.
[c] The J^π values have been obtained from Ref. 3 and from the findings of the present work.
[d] Reference 4.
[e] Present work.
[f] Calculated for $J=\frac{1}{2}$.
[g] Calculated for $J=\frac{3}{2}$.
[h] Calculated for $J=\frac{5}{2}$.

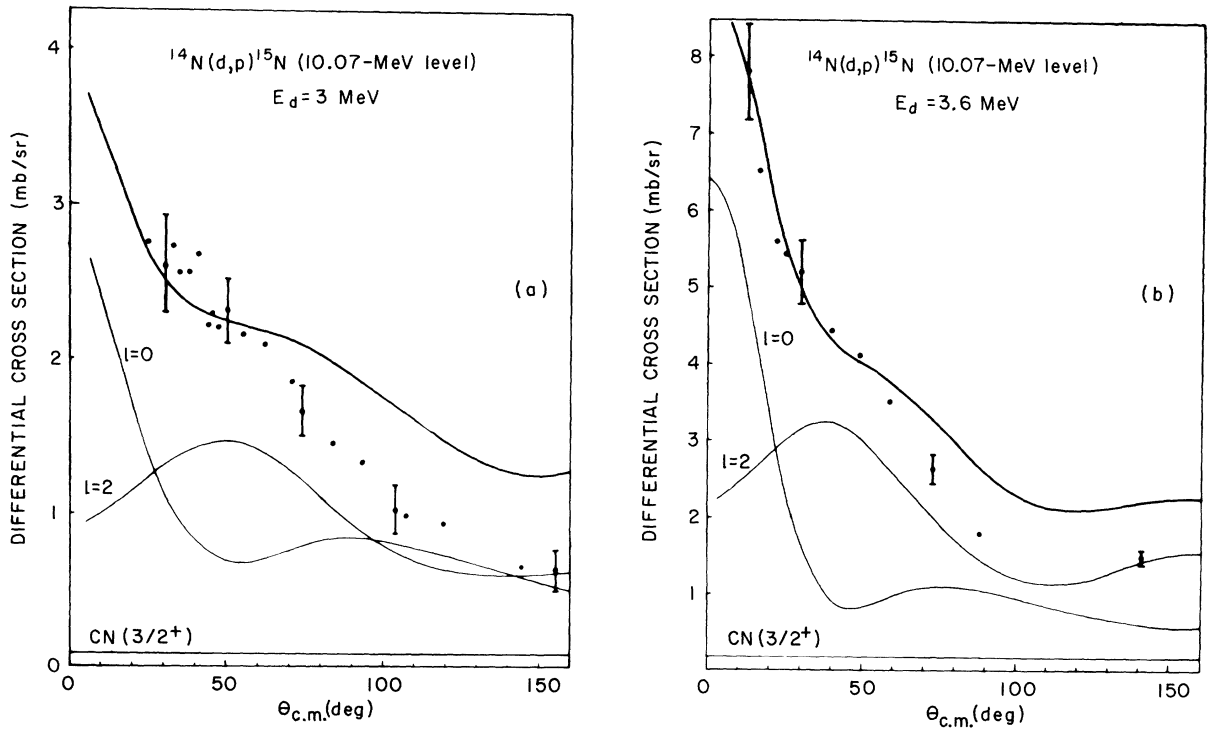

FIG. 9. $^{14}N(d,p)^{15}N$ angular distributions for the $\frac{3}{2}^+$ 10.07-MeV level at $E_d=3$ and 3.6 MeV. The solid curves represent the sum of $l_n=0$ and $l_n=2$ DWBA fits (including the Hauser-Feshbach contribution) calculated for (D_1, P_1) combination.

extracted spectroscopic factors S are listed in Table II. The spectroscopic factors for the 10.07-MeV state are in reasonable agreement with the values obtained by Phillips and Jacobs[4] at $\bar{E}_d = 8$ MeV.

VII. CONCLUSIONS

A. Comparison with Theory

The results obtained from this work may be compared with the predictions of the weak-coupling model for the positive- and negative-parity states of the $A = 15$ nuclei[1,2] (Fig. 1). These calculations have been performed for the ^{15}O case.

The 9.05-MeV state has been identified with the third $\frac{1}{2}^+$ state suggested by Lie, Engeland, and Dahll[1] at 7.65 MeV. The calculated γ decays are in good agreement with the experimental data. However, the 9.05-MeV state is preferentially populated in single-particle transfer ^{14}N(d,p)^{15}N; the experiment gives 0.15 for the spectroscopic factor, when the model wave function contains a negligible amount of the ^{14}N ground state coupled to a s-d particle. Finally, the spin of the 9.05-MeV state is not known with certainty; a $J = \frac{3}{2}$ assignment[21] cannot be excluded and, in this case, the correspondence with the model has to be reconsidered.

The $\frac{5}{2}^+$ 9.155-MeV state is identified with the third $\frac{5}{2}^+$ state predicted by Lie, Engeland, and Dahll[1] at 7.75 MeV. The experimental value of the spectroscopic factor is 0.13 in agreement with the value 0.10 predicted by weak-coupling calculations.

The $\frac{3}{2}^+$ 10.07-MeV state has the predominant 1p-2h components. This state corresponds to the third $\frac{3}{2}^+$ state predicted by Lie, Engeland, and Dahll[1] at 8.92 MeV; $l_n = 0$ and $l_n = 2$ experimental spectroscopic factors are 0.15 and 0.64 while Lie, Engeland, and Dahall[1] give 0.06 and 0.64, respectively.

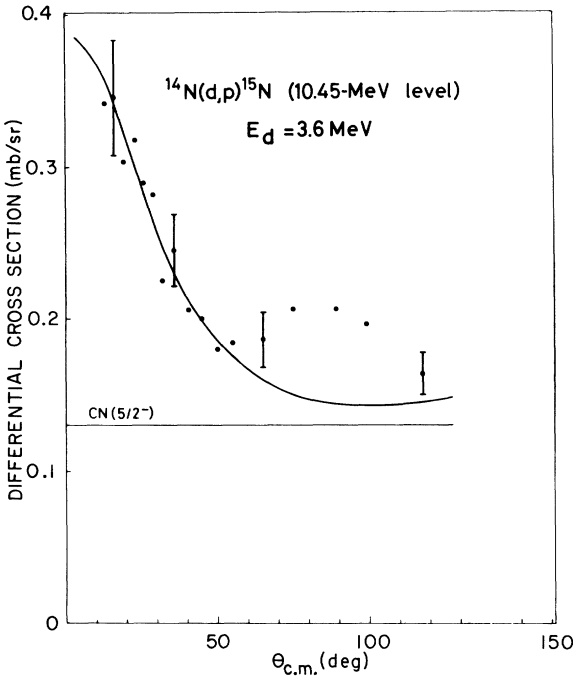

FIG. 10. ^{14}N(d,p)^{15}N angular distributions for the 10.45-MeV level at $E_d = 3.6$ MeV. The solid curve represents $l_n = 1$ DWBA fit (including the Hauser-Feshbach contribution) calculated for (D_1, P_1) combination.

The negative-parity states for $A = 15$ investigated in a weak-coupling model[2] contain a negligible amount of 1p-2h components, in agreement with the very low values ($\lesssim 0.04$) of experimental spectroscopic factors measured here. The $\frac{3}{2}^-$ 9.152-,

TABLE III. Comparison of the reduced widths γ_n^2 and γ_p^2 for the isobaric analog states of ^{15}N and ^{15}O.

E_x (^{15}N) [a] (MeV)	J^π (^{15}N) [b]	E_x (^{15}O) [a] (MeV)	J^π (^{15}O)	Γ_p (keV)	γ_n^2 [e] (keV)	γ_p^2 [e] (keV)	γ_n^2/γ_p^2
9.05	$(\frac{1}{2}, \frac{3}{2})^+$	8.74	$\frac{1}{2}^+$ [c]	34 [c]	126	38	3.3
9.152	$\frac{3}{2}^-$	8.98	$(\frac{1}{2}, \frac{3}{2})^-$ [c]	4.2 [c]	17	8.4	2
9.155	$\frac{5}{2}^+$	8.92	$\frac{5}{2}^+$ [d]	3.5 [d]	59	48	1.2
9.22	$\frac{1}{2}^-$	8.92	$\frac{1}{2}^-$ [d]	9 [d]	23	19	1.2
9.76	$\frac{5}{2}^-$	9.48	$\frac{5}{2}^-$ [c]	10.8 [c]	12	12	1
10.07	$\frac{3}{2}^+$	9.50	$\frac{3}{2}^+$ [c]	300 [c]	140(0) 390(2)	102(0) 650(2)	1.4 0.6

[a] Reference 3.
[b] Reference 3 and this work.
[c] Reference 3.
[d] Reference 24.
[e] Calculated with $R = 4.8$ fm.

$\frac{1}{2}^-$ 9.22-, $\frac{5}{2}^-$ 9.76-MeV states are identified with the states predicted by Lie and Engeland[2] at 9.45, 8.57, and 9.77 MeV (Fig. 1). Thus, the connection between states of ^{15}N of known spin and parity and their counterparts in the weak-coupling model appears fairly well established.

B. Comparison with the Isobaric Analog States of ^{15}O

The correspondence between the states of ^{15}N and the isobaric analog states in ^{15}O is well known below $E_x < 8.58$ MeV[3] in ^{15}N and is indicated in Fig. 1 by solid lines. The analog states of those presently investigated in ^{15}N are expected at $E_x \geq 8.74$ MeV in ^{15}O and hence can be observed in the elastic scattering of protons by ^{14}N. Using the recently reported results[23,24] of a ^{14}N$(p,p)^{14}$N study, the correspondence indicated by dashed lines is suggested here (Fig. 1).

If this correspondence is correct, the neutron reduced width $\gamma_n^2(R)$ is related to the proton reduced width γ_p^2 by the relation

$$\gamma_n^2(R) = \gamma_p^2(R) \tag{3}$$

using the assumption of charge independence in the interior region of the nucleus. The relation between the conventional R matrix reduced width and the spectroscopic factors S measured above is

$$\gamma_n^2(R) = \left(\frac{\hbar^2}{2mR}\right) u_n^2(R) S , \tag{4}$$

where $u_n(r)$ is the neutron radial wave function calculated by solving the Schrödinger equation for a bound neutron in a Woods-Saxon real well and normalized such that

$$\int_0^\infty u_n^2(r)dr = 1 .$$

The proton reduced width γ_p^2 is related to the experimentally extracted width Γ_p by

$$\gamma_p^2(R) = \Gamma_p / P_l , \tag{5}$$

where P_l is the penetration factor defined as

$$P_l(kR) = 2kR/F_l^2 + G_l^2 .$$

The γ_n^2 and γ_p^2 reduced widths have been obtained from Eqs. (4) and (5), respectively, using $R = 4.80$ fm and are listed in Table III. The proton widths Γ_p are extracted from Refs. 23 and 24. As can be seen in Table III, the deviation of γ_n^2/γ_p^2 from unity is well within the experimental uncertainties except in the case of the 9.05-MeV state in ^{15}N and the 8.74-MeV state in ^{15}O. Thus, this last correspondence is uncertain and this is confirmed by the experimental γ decays which differ considerably for these states. For the other states in ^{15}N, the correspondence suggested in Fig. 1 is confirmed by these results.

The analog of the $\frac{5}{2}^+$ 9.155-MeV state of ^{15}N is the $\frac{5}{2}^+$ member of a doublet recently observed in ^{15}O at 8.920 MeV by Lambert *et al.*,[24] the other, $\frac{1}{2}^-$ member of this doublet corresponding probably to the 9.22-MeV state in ^{15}N. The $\frac{3}{2}^-$ 8.98-MeV state of ^{15}O is likely to be the analog of the $\frac{3}{2}^-$ 9.152-MeV state of ^{15}N. Finally, Table III confirms the well-established correspondence between the $\frac{5}{2}^-$ 9.76- and $\frac{3}{2}^+$ 10.07-MeV states of ^{15}N and their analog states in ^{15}O at 9.48 and 9.49 MeV, respectively. The $\frac{7}{2}$ 9.83-MeV state in ^{15}N could correspond to the $(\frac{7}{2}, \frac{9}{2})^-$ 9.67-MeV state in ^{15}O. The $(\frac{1}{2}, \frac{3}{2})^{(+)}$ state of ^{15}N at 9.93 MeV alone has no counterpart, but the parity of this state is still uncertain and should be established before any discussion.

[1] S. Lie, T. Engeland, and G. Dahll, Nucl. Phys. A156, 449 (1970).
[2] S. Lie and T. Engeland, Nucl. Phys. A169, 617 (1971).
[3] F. Ajzenberg-Selove, Nucl. Phys. A152, 1 (1970).
[4] G. W. Phillips and W. W. Jacobs, Phys. Rev. 184, 1052 (1969).
[5] J. P. Cremet, M. Lambert, G. Lefevre, and L. Rais, Rev. Phys. 1, 267 (1966).
[6] M. Schmitt, J. Herry, and Y. Flamant, Nucl. Instr. Methods 91, 321 (1971).
[7] P. E. Hodgson and D. Wilmore, Proc. Phys. Soc. (London) 90, 361 (1967).
[8] V. Gomes Porto, N. Ueta, R. A. Douglas, O. Sala, D. Wilmore, B. A. Robson, and P. E. Hodgson, Nucl. Phys. A136, 385 (1969).
[9] C. Morand, Thèse de Doctorat de 3ème Cycle, Alger, 1970 (unpublished).
[10] H. Beaumevieille, M. Lambert, M. Yaker, A. Amokrane, and Nguyen Van Sen, Nucl. Phys. A125, 568 (1969).
[11] O. Dietzch, R. A. Douglas, E. Farrely Pessoa, V. Gomes Porto, E. W. Hamburger, T. Polga, O. Sala, S. M. Perez, and P. E. Hodgson, Nucl. Phys. A114, 330 (1968).
[12] A. Gallmann, P. Fintz, and P. E. Hodgson, Nucl. Phys. 82, 161 (1966).
[13] W. R. Smith and E. V. Ivash, Phys. Rev. 131, 304 (1963).
[14] D. Wilmore and P. E. Hodgson, Nucl. Phys. 55, 673 (1964).
[15] Nguyen Van Sen, Thèse de Doctorat d'Etat, Grenoble, 1967 (unpublished).
[16] E. K. Warburton, J. W. Olness, and D. E. Alburger, Phys. Rev. 140, B1202 (1965).
[17] E. K. Warburton and J. W. Olness, Phys. Rev. 147, 698 (1966).

[18]G. W. Phillips, F. C. Young, and J. B. Marion, Phys. Rev. 159, 891 (1967).
[19]T. S. Green and R. Middleton, Proc. Phys. Soc. (London) A69, 28 (1955).
[20]C. E. Steerman and F. C. Young, Technical Report No. 72-006 (1971), University of Maryland (unpublished); and to be published.
[21]H. E. Siefken, P. M. Cokburn, and R. W. Krone, Nucl. Phys. A128, 162 (1969).
[22]N. Austern, *Direct Nuclear Reaction Theories* (Wiley, New York, 1970), p. 162.
[23]M. Lambert and M. Durand, Phys. Letters 24B, 287 (1967); J. Phys. 28, 349 (1969).
[24]M. Lambert, O. Bersillon, B. Chambon, D. Drain, and J. L. Vidal, Lettere Nuovo Cimento 23, 1193 (1971).

PHYSICAL REVIEW C VOLUME 6, NUMBER 6 DECEMBER 1972

Equations for Four-Particle Scattering*

Ian H. Sloan†
Department of Physics and Astronomy, University of Maryland, College Park, Maryland 20742
(Received 17 July 1972)

Four-particle scattering equations are obtained that are analogous to the Lovelace or Alt-Grassberger-Sandhas equations in the three-particle case: They are equations whose kernel is connected after one iteration, in which the unknown quantities are the transition operators for the various elastic, inelastic, and rearrangement processes. The equations couple together only the transitions to the two-body channels, exactly as in the three-particle analogs, so that there are seven coupled integral equations, corresponding to the seven two-body channels (four of nucleon+triton type, and three of deuteron+deuteron type). Transition operators to the three- and four-body channels appear as integrals over the transition operators to the two-body channels.

I. INTRODUCTION

The celebrated Faddeev equations[1] for the three-particle problem have the essential property that the iterated kernel is connected (for complex energies), so that at least in principle they can be solved with ordinary numerical techniques. However, the solutions of the original Faddeev equations are not related in any very simple way to the amplitudes for the various elastic, inelastic, and rearrangement processes that can occur. For this reason, the variants of the Faddeev equations proposed by Lovelace[2] and by Alt, Grassberger, and Sandhas[3] have often been preferred in practice.

The subject of this paper is the four-particle scattering problem, and the principal aim is to obtain four-particle equivalents of the Lovelace-AGS equations, i.e., equations with connected kernels in which the quantities that appear are the transition operators for the various scattering processes. As far as we are aware, such equations have not previously been given. These equations have the advantage that they make the formulation of scattering problems much more direct, and we believe might bring the simplest four-particle problems within the range of modern computers.

The four-particle problem is considerably more complicated than the three-particle, and it is therefore hardly surprising that it has not reached the same stage of development. However, many authors[4-11] have written down connected equations for the four-particle problem, using a variety of techniques[12] to cure the disconnectedness problem. In only one case, that of the Yakubovskiĭ equations,[11] has it been proved that the solutions of the homogeneous equation at negative energies are always solutions of the Schrödinger equation. It is therefore possible for the other formulations that the homogeneous equations have additional solutions, which might cause difficulties in bound-state studies. On the other hand, the Yakubovskiĭ equations, which are sets of eighteen coupled equations, appear extremely difficult to use in any practical calculation. And if one's interest is in scattering rather than in the bound states, as in the present work, then the possible ambiguities in bound-state calculations are not of direct concern.

The four-particle equations of greatest importance for the present work are those obtained independently by Rosenberg,[7] Mitra *et al.*,[8] Takahashi and Mishima,[9] and Alessandrini.[10] These are sets of six coupled equations (one for each of the six pairs), in which the kernels are the connected parts of the amplitudes for the three-particle subsystems, and also for the subsystems consisting of two noninteracting pairs. The equations we obtain at the end of this paper (which are sets of *seven* coupled equations) are related to these